AD-A151 451 DYNAMIC CRACK CURVING AND BRANCHING UNDER BIAXIAL LOADING(U) WASHINGTON UNIV SEATTLE DEPT OF MECHANICAL ENGINEERING J S HAWONG ET AL. FEB 85 UWA/DME/TR-85/50 1/1

UNCLASSIFIED N00014-76-C-0060 F/G 20/11 NL

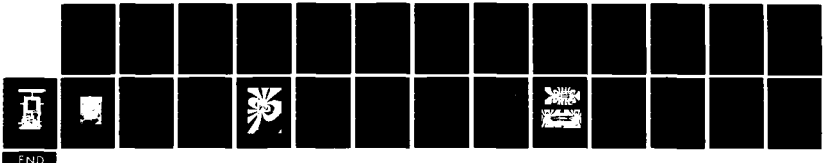

END

FILMED

DTIC

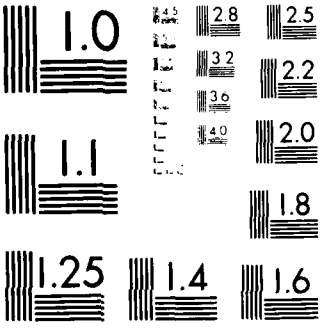

Office of Naval Research

Contract N00014-76-0060 NR 064-478

Technical Report No. UWA/DME/TR-85/50

DYNAMIC CRACK CURVING AND BRANCHING UNDER BIAXIAL LOADING

by

J. S. Hawong, A. S. Kobayashi, M. S. Dadkhah, B. S.-J. Kang and M. Ramulu

February 1985

The research reported in this technical report was made possible through support extended to the Department of Mechanical Engineering, University of Washington, by the Office of Naval Research under Contract N00014-76-C-0060 NR 064-478. Reproduction in whole or in part is permitted for any purpose of the United States Government.

Department of Mechanical Engineering

College of Engineering

University of Washington

Dynamic Crack Curving and Branching Under Biaxial Loading

J. S. Hawong*, A. S. Kobayashi, M. S. Dadkhah, B. S.-J. Kang and M. Ramulu
University of Washington
Department of Mechanical Engineering
Seattle, Washington 98195

ABSTRACT

A 16 spark-gap camera was used to record the dynamic photoelastic patterns of ten centrally cracked, Homalite-100 specimens which fractured under ten biaxial stress ratios ranging from 3.7 to 0. The dynamic photoelastic patterns of curved cracks were used to verify the previously developed dynamic crack curving criterion. Cracks, which immediately curved upon propagation in three specimens under high biaxial loadings, were used to verify the static counterpart of the dynamic crack curving criterion. A previously developed dynamic crack branching criterion was verified by the dynamic photoelastic results involving cracks which eventually branched under low biaxial loadings.

INTRODUCTION

Dynamic crack curving and branching represent one aspect of dynamic crack propagation behaviors which has been the subject of numerous theoretical [1-5] and experimental [6-9] investigations. The biaxial load effects on static and quasistatic fracture have also been the subject of theoretical and experimental studies [10-12]. The purpose of this paper is to report our

*On leave from Yeungnam University, Gyongsang, Republic of Korea at the time of this research.

studies on the combination of these two, namely, dynamic crack curving and branching under various biaxial loading conditions.

The crack curving criteria [3] referred to in this paper is a micro-mechanic model of continuous micro-flaw growth and coalescence in the vicinity of the propagating crack tip. A similar model based on qualitative evidences has also been proposed [13]. The model assumes that the crack kinks or bifurcates, when an off-axis micro-flaw connects with the crack tip. It is the dynamic extension of the crack curving criterion proposed by Streit and Finnie [5]. This dynamic crack curving criterion has been used to predict the crack kinking angle of a propagating crack under pure mode I as well as mixed mode conditions [3]. The crack branching criterion [4] on the other hand, requires a critical stress intensity factor to trigger crack branching and a crack curving criterion for predicting the crack branching angle. The objective of this paper is to provide further evidences in support of the dynamic crack curving and branching criteria under biaxial loadings.

DYNAMIC CRACK CURVING CRITERION

The authors have used in the past, both the maximum circumferential stress criterion [3] and the minimum strain energy density criterion [14] to predict crack curving. The crack curving angles predicted by using either of the two fracture criteria are nearly identical for smaller values of mode II stress intensity factor, K_{II}, and thus only the circumferential stress criterion will be used in this paper. The near field circumferential stress, $\sigma_{\theta\theta}$, of a mixed-mode crack-tip propagating at constant velocity is a function of the modes I and II dynamic stress intensity factors, K_I and K_{II}, and the remote stress or the non-singular stress acting in the direction of crack propagation, σ_{ox}. $\sigma_{\theta\theta}$ is also a function of the crack velocity, c_1,

dilatational and distortional stress wave velocities, c_1 and c_2, along with the other higher order terms (HOT) in the crack tip stress field. Crack curving occurs when $\sigma_{\theta\theta}$ reaches a maximum value at an inclination of θ and a distance of r away from the propagating crack. This extremum condition for yields a functional relation between the r and θ values. By setting $\theta = 0$ in this relation under pure mode I loading, i.e. $K_{II} = 0$, a characteristic radial distance, r_o, for self-similar crack extension is obtained in terms of K_I, σ_{ox}, c, c_1 and c_2 and the higher order terms, HOT.

This crack instability criterion, which is a dynamic extension to static crack directional instability criterion of Streit and Finnie [5], assumes that the crack will propagate straight when the above characteristic distance of r_o is larger than a critical material parameter of r_c. When r_o is less than r_c, the crack suddenly becomes unstable and will veer off to the θ_c direction which is determined from the extremum condition. Detailed studies on the variations in this crack kinking angle with respect to variations in fracture parameters are given in References [3, 14].

DYNAMIC CRACK BRANCHING CRITERION

The dynamic crack branching criterion requires as a necessary condition, sufficient released strain energy for generating simultaneously, multiple cracks. Thus, a critical stress intensity factor, K_{Ib}, is implicated in this necessary condition.

In order to propagate the multiple cracks simultaneously, these cracks must branch away from the original self-similar crack propagation path. Thus, crack curving is introduced as a sufficiency condition. The crack branching criterion can then be summarized as:

$K_I > K_{Ib}$	Necessary condition
$r_o < r_c$	Sufficient condition

The crack kinking angle determined from the above sufficiency condition is one half of the crack branching angle.

FRACTURE UNDER BIAXIAL LOADING

Biaxial loading of fracture specimens have been reported to influence, among others, the apparent fracture toughness, fatigue crack propagation rate, plastic zone size and the direction of crack propagation. Of particular interest to this investigation is the predicted direction of the initial crack extension of a centrally cracked plate under biaxial loading in Reference [12]. Using the maximum circumferential stress criterion, Liebowitz et al showed that the directional instability of a central crack occurs when

$$r_o \frac{\sqrt{\sigma_{ox}}}{K_I} > 0.1493\ (B-1) \qquad \text{when } B > 1.0$$

where r_o is a small but unspecified characteristic distance from the crack tip and B is the ratio of the biaxial loads, i.e., $B = F_x/F_y$. Since this crack kinking criterion corresponds to the static counterpart of the authors' dynamic crack curving criterion, both criteria will be used to evaluate the crack kinking data obtained in fracturing centrally cracked plates with blunt notches and under biaxial loadings.

EXPERIMENTAL AND DATA REDUCTION PROCEDURES

Dynamic photoelasticity was used to determine the dynamic stress intensity factors in a fracturing Homalite-100 specimen which was loaded in a biaxial testing machine. The transient isochromatics surrounding the propagating cracks were recorded by a sixteen spark-gap Cranz-Schardin camera. The spark is sensed by an EG&G Lite-mike and recorded on a Biomation 2805M wave form recorder.

The biaxial testing machine consists of two sets of two oppositely mounted hydraulic cylinders, which allows the center of the specimen to remain stationary as shown in Figure 1. Each set has its own dented control valve, accumulator, handpump and pilot operated check valve. The two hydraulic systems can be operated independently, in tension and in compression, as well as simultaneously while maintaining a fixed load ratio. The two loads, which are measured by two load cells and through the necessary strain gage conditioners and amplifiers, are recorded both on a Brush recorder and on a Biomation 2805M wave form recorder.

Figure 2 shows a 16.4 mm thick, fractured Homalite-100 cruciform specimen with a central starter crack of 50 mm length in a test area of approximately 254 x 254 mm. The elastodynamic properties of Homalite-100 were determined by a split Hopkinson bar tester which yielded modulus of elasticity, Poisson ratio and stress optical constant of 4.27 GPa, 0.357 and 32.8 MPa-mm/fr, respectively at a strain rate of about 2×10^2 1/sec.

The least square procedure [15,16] was used to determine the fracture parameters, i.e. the stress intensity factors, K_I and K_{II}, where applicable, the remote stress component, σ_{ox}, and two additional higher order terms (HOT) of Mode I and Model II, A_3 and B_3, respectively from the transient isochromatics. Convergence of this procedure was verified for each computation by the goodness of fit between the experimentally obtained isochromatics and those reconstructed from computed dynamic fracture parameters.

RESULTS

A total of ten specimens with different biaxial load ratios, as shown in Figure 3, were tested. The ratios of applied load, which are parallel and normal to the central crack, ranged from B = 3.7 - 0.

The 45 degree crack in Specimen No. DH073084, which was loaded to failure under nearly equal biaxial load, i.e. B = 1.07, propagated in a self similar straight line, thus indicating that the biaxial testing machine generated a uniform stress field. On the other hand, the 45 degree crack in Specimen No. DH080284, which failed at a biaxial load ratio of B = 1.53, immediately curved upon propagation as expected. Dynamic crack curving, which occurred in specimen under low biaxial load ratios of B = 1.6, 1.33 and 1.16 in Specimen Nos. DH072084, DH062284 and DH062584, respectively, were also used to evaluate the dynamic crack curving criterion. Cracks emanating from the horizontal cracks in Specimens Nos. DH071684, DH071784 and DH071984 under biaxial load ratios of B = 3.7, 3.06 and 2.6, respectively immediately curved upon propagation and before the camera could be triggered. These results were used to evaluate the authors [3] and Liebowitz et al [12] static crack curving criteria. Figure 4 shows Specimen No. DH071784 in which the crack branched immediately upon propagation from two sharp starter crack tips. The crack branching data which occurred after crack curving in three specimens, which includes the above Specimen No. DH071784, were used to evaluate the crack branching criterion. Selected results are discussed in the following.

Figure 5a shows the dynamic photoelastic fringe patterns associated with Frame No. 9 of Specimen No. DH072084. Figure 5b shows the data points used in evaluating K_I, K_{II}, σ_{ox}, A_3 and B_3, as well as the reconstructed isochromatics using these crack tip parameters. Figures 6a and 6b shows the variations in K_I, K_{II} and σ_{ox} in the right and left cracks of Specimen No. DH072084.

Figure 7 shows the crack path which resulted in a crack branching in Specimen No. DH072084. Also shown in Figure 7 is the corresponding measured and predicted crack curving angles along the crack path. The latter was computed by substituting the resultant K_I, K_{II} and σ_{ox} and the two higher order terms, A_3 and B_3, into the crack curving criterion.

Figure 8 shows two frames of the dynamic isochromatics prior to and after crack branching in Specimen No. MDO12884. Figures 9a and 9b show the variations in K_I, and σ_{ox} before crack branching of the left and right cracks. Extrapolated K_I and σ_{ox} values were then used to determine the dynamic crack branching stress intensity factor as well as the branching angle.

Table 1 shows the measured and computed crack curving angles immediately after crack propagation in the five specimens shown in Figure 3. Both the authors' [3] and Liebowitz et al [12] procedures were used to estimate the initial crack curving angles. Good agreements between all theoretical and experimental results are noted.

Table 2 shows the measured crack branching stress intensity factor as well as the measured and estimated crack branching angles in four specimens. At the lower biaxial ratios, $B < 1.0$, the experimentally observed crack branching angles are within 24 - 44 degrees as reported by others [4,8,16-18] under uniaxial loading. The crack branching angles, however, increased with increase in the biaxiality ratios. It is also interesting to note that a meager 13% increase in the branching stress intensity factor, K_{Ib}, resulted in multiple crack branching.

The two Tables, I and II, show that the curving and branching angles can be predicted with reasonable accuracy. Regardless of the biaxial loading ratio and the branching crack length, the branching stress intensity factor of 2.0 MPa$\sqrt{m}$ is obtained for Homalite-100 and is in good agreement with the results reported in Reference [4].

CONCLUSIONS

1. Dynamic crack curving branching criterion proposed by the authors successfully predicted the crack curving and crack branching angle under σ_{ox} extremes observed in biaxial loading.

2. A crack branching stress intensity factor of $K_{Ib} = 2.0$ MPa$\sqrt{m}$ was determined for this Homalite-100 sheet and is independent of biaxial loading ratio.

ACKNOWLEDGEMENT

The work reported here was obtained under ONR Contract NO-0014-76-C-000 NR-064-478. The authors wish to acknowledge the support and encouragement of Dr. Y. Rajapakse, ONR, during the course of this investigation.

REFERENCES

1. Cotterell, B., "Notes on the Paths and Stability of Cracks," International Journal of Fracture Mechanics, Vol. 2, No. 2, 1966, pp. 526-533.

2. Cotterell, B. and Rice, J. R., "Slightly Curved or Kinked Cracks" International Journal of Fracture, Vol. 11, no. 2, 1981, pp. 155-164.

3. Ramulu, M. and Kobayashi, A. S., "Dynamic Crack Curving - A Photoelastic Evaluation," Experimental Mechanics, Vol. 23, March 1983, pp. 1-9.

4. Ramulu, M., Kobayashi, A. S. and Kang, B. S. J., "Dynamic Crack Branching - A Photoelastic Evaluation,", Fracture Mechanics: Fifteenth Symposium, ed. R. J. Sanford, ASTM STP, 833, 1984, pp. 130-148.

5. Streit, R. and Finnie, I., "An Experimental Investigation of Crack Path Directional Stability," Experimental Mechanics, Vol. 20, Jan. 1980, pp. 17-23.

6. Rossmanith, H. P., "Crack Branching of Brittle Materials, Part I," University of Maryland Report, 1977-1980.

7. Dally, J. W., "Dynamic Photoelastic Studies of Experimental Mechanics, Vol. 19, No. 10, 1979, pp. 349-367.

8. Congleton, J., "Practical Applications of Crack-Branching Measurements," Dynamic Crack Propagation, ed. by G. C. Sih, Noordhoff Int. Pub., Leyden, 1973, pp. 427-438.

9. Shannon, R. W. E. and Wells, A. S., "A Study of Ductile Crack Propagation in Gas Pressurized Pipeline," Proceedings of International Symposium on Pipeline, Paper No. 17, Newcastle upon Tyne, Mar. 1974.

10. Leevers, P. S., Radon, J. C. and Culver, "Crack Growth in Plastic Panels Under Biaxial Stress," Polymer, Vol. 17, 1976, pp. 627-632.

11. Kitagawa, H. and Yuuki, R., "Analysis of Branched Cracks Under Biaxial Stresses," Fracture 1977, Vol. 3, ICF4, Waterloo, Canada, pp. 201-213.

12. Liebowitz, H., Lee, J. D., and Eftis, J., "Biaxial Load Effects in Fracture Mechanics," Engineering Fracture Mechanics, 1978, Vol. 10, pp.315-335.

13. Ravi-Chandar, K. and Knauss, W. G., "An Experimental Investigation into Dynamic Fracture: III. On Steady State Crack Propagation and Branching," International Journal of Fracture, Vol. 26, 1984, pp. 141-154.

14. Ramulu, M. and Kobayashi, A. S., "Strain Energy Density Fracture Criterion in Elasto-dynamic Mixed Model Crack Propagation" Engineering Fracture Mechanics, vol. 18, no. 6, pp. 1087-1098, 1983.

15. Sanford, R. J. and Dally, J. W., "A General Method for Determining Mixed Mode Stress Intensity Factors from Isochromatic Fringe Patterns," Engineering Fracture Mechanics, 11, 1979, pp. 621-633.

16. Kobayashi, A. S. and Ramulu, M., "Dynamic Stress Intensity Factors for Unsymmetric Dynamic Isochromatics," Experimental Mechanics, vol. 21, no. 1, pp. 41-48, 1981.

17. Kalthoff, J. F., "On the Propagation of Bifurcated Cracks," Dynamic Crack Propagation, ed. by G. C. Sih, Noordhoff Int. Pub., 1973, pp. 449-458.

18. Ramulu, M. Kobayashi, A. S., Kang, B. S. J. and Barker, D. C., "Further Studies on Dynamic Crack Branching," Experimental Mechanics, vol. 23, no. 4, pp. 431-437, 1983.

TABLE I

TEST SPECIMEN NO.	Biaxial Load Ratio B	CRACK CURVING ANGLE (in degrees) Measured θ_m	Predicted θ_t Ramulu et al	Predicted θ_t Liebowitz et al
DH071684	3.7	76	71.7	72.5
DH071784	3.05	67	66.2	65.7
DH071984	2.6	54	52	56.5
DH072084	1.6	5	0	0
DH080284	1.53	30	32.5	29

TABLE 2
SUMMARY OF CRACK BRANCHING DATA UNDER BIAXIAL LOADING

SPECIMEN NO.	Biaxial Load Ratio B	K_{Ib} (MPa$\sqrt{m}$)	CRACK BRANCHING ANGLE IN DEGREES Measured θ_m	Estimated θ_e
MD012284R	0.0	1.87	28	40
MD012284L		1.98	24	22
MD012884R	0.33	1.98	44	44
MD012884L		2.05	40.5	40
DH072084R	1.6	2.0	49	-
DH072084L**		2.1	-	-
DH071984R	2.6	1.98	50	-
DH071984L**		2.12	-	-
DH071784R*	3.05	-	-	-
DH071784L**		2.12	-	-
Average		2.02		

L: Left Crack
R: Right Crack
* No Branching
** Multiple Branching

20. ABSTRACT (Cont.)

crack branching criterion was verified by the dynamic photoelastic results involving propagation cracks which eventually branched under low biaxial loadings.

Unclassified

SECURITY CLASSIFICATION OF THIS PAGE (When Data Entered)

REPORT DOCUMENTATION PAGE		READ INSTRUCTIONS BEFORE COMPLETING FORM
1 REPORT NUMBER UWA/DME/TR-85/50	2. GOVT ACCESSION NO. AD-A151 477	3 RECIPIENT'S CATALOG NUMBER
4 TITLE (and Subtitle) Dynamic Crack Curving and Branching Under Biaxial Loading		5. TYPE OF REPORT & PERIOD COVERED UWA/DME/TR-85/50 6. PERFORMING ORG. REPORT NUMBER
7. AUTHOR(s) J. S. Hawong, A. S. Kobayashi, M. S. Dadkhah, B. S. J. Kang and M. Ramulu		8. CONTRACT OR GRANT NUMBER(s) N00014-76-C-0060
9 PERFORMING ORGANIZATION NAME AND ADDRESS Dept. of Mechanical Engineering, FU-10 University of Washington Seattle, Washington 98195		10. PROGRAM ELEMENT, PROJECT, TASK AREA & WORK UNIT NUMBERS NR 064-478
11. CONTROLLING OFFICE NAME AND ADDRESS Office of Naval Research Arlington, VA 22217		12. REPORT DATE February 1985 13. NUMBER OF PAGES
14 MONITORING AGENCY NAME & ADDRESS(if different from Controlling Office)		15. SECURITY CLASS. (of this report) unclassified 15a. DECLASSIFICATION/DOWNGRADING SCHEDULE

16 DISTRIBUTION STATEMENT (of this Report)

Unlimited

17. DISTRIBUTION STATEMENT (of the abstract entered in Block 20, if different from Report)

18 SUPPLEMENTARY NOTES

19 KEY WORDS (Continue on reverse side if necessary and identify by block number)

Dynamic fracture, crack branching biaxial loading, curving and branching angles, dynamic photoelasticity

20 ABSTRACT (Continue on reverse side if necessary and identify by block number)

A 16 spark-gap camera was used to record the dynamic photoelastic patterns of ten centrally cracked, Homalite-100 specimens which fractured under ten biaxial stress ratios ranging from 3.7 to 0. The dynamic photoelastic patterns of curved cracks were used to verify the previously developed dynamic crack curving criterion. Cracks, which immediately curved upon propagation in the specimens under high biaxial loadings, were used to verify the static counterpart of the dynamic crack curving criterion. A previously developed dynamic

DD FORM 1 JAN 73 1473 EDITION OF 1 NOV 65 IS OBSOLETE
S/N 0102-014-6601

Unclassified

SECURITY CLASSIFICATION OF THIS PAGE (When Data Entered)

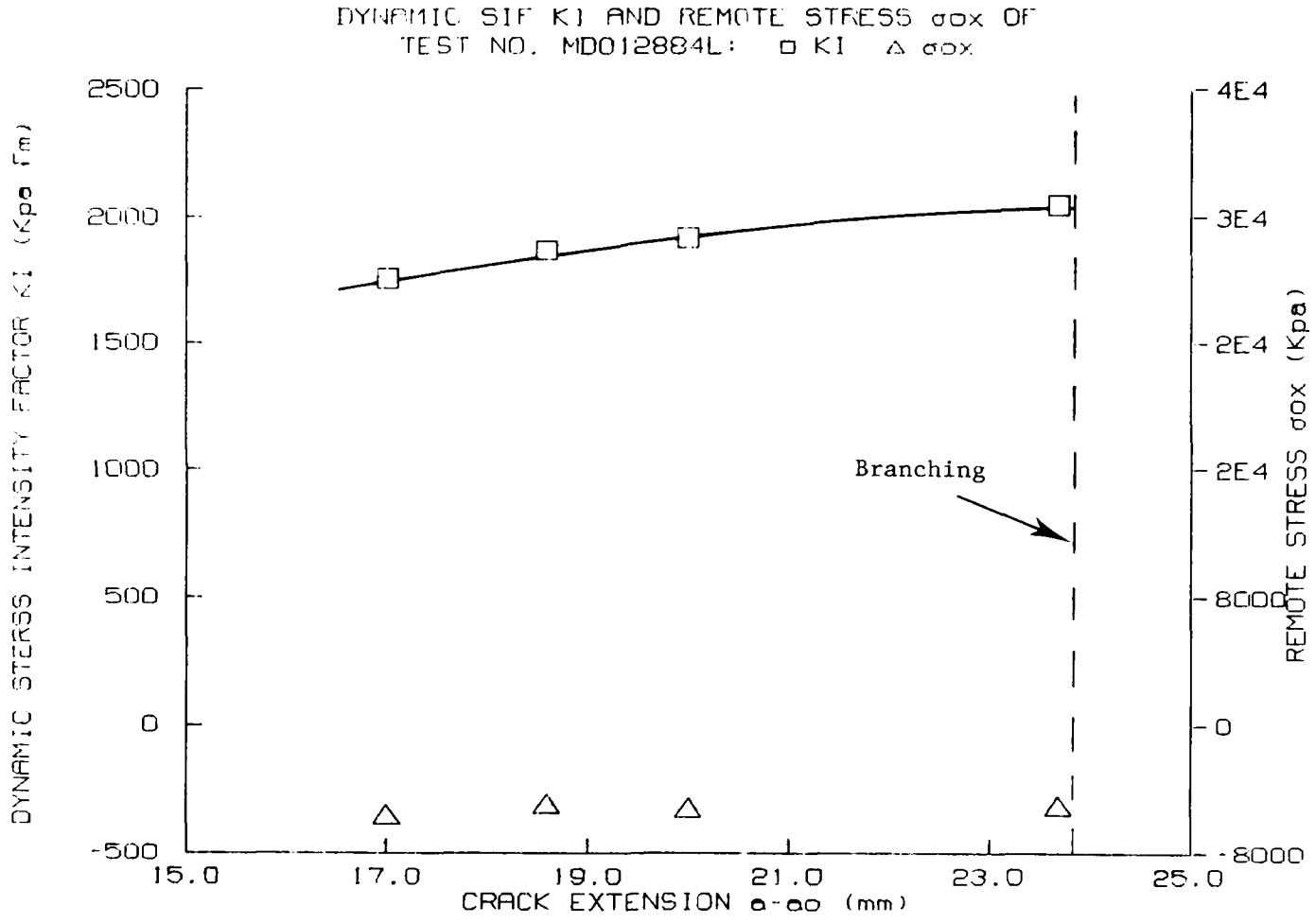

Figure 9b. K_I and σ_{ox} Variations Along Left Crack Prior to Branching

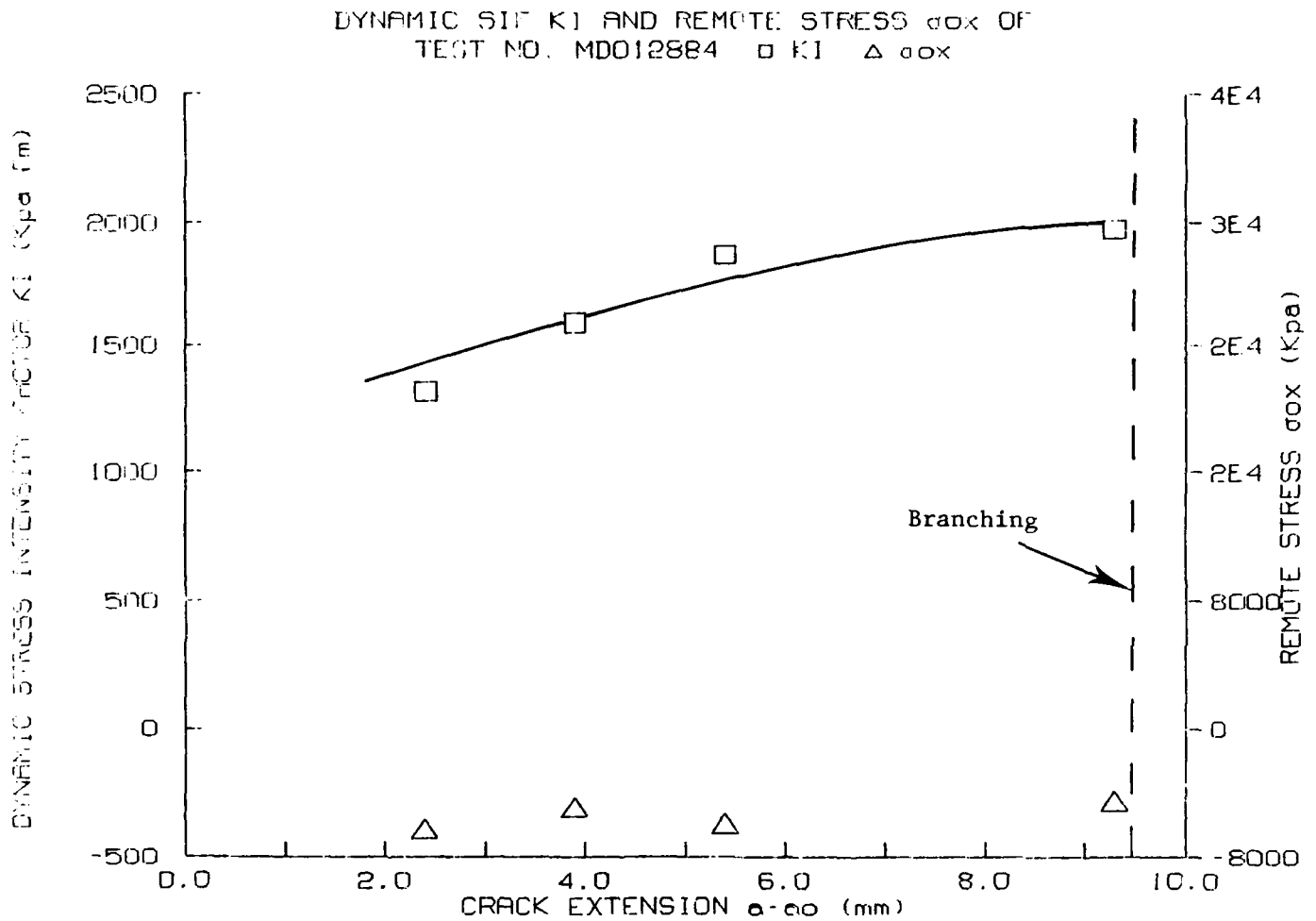

Figure 9a. K_I and σ_{ox} Variations Along Right Crack Prior to Branching

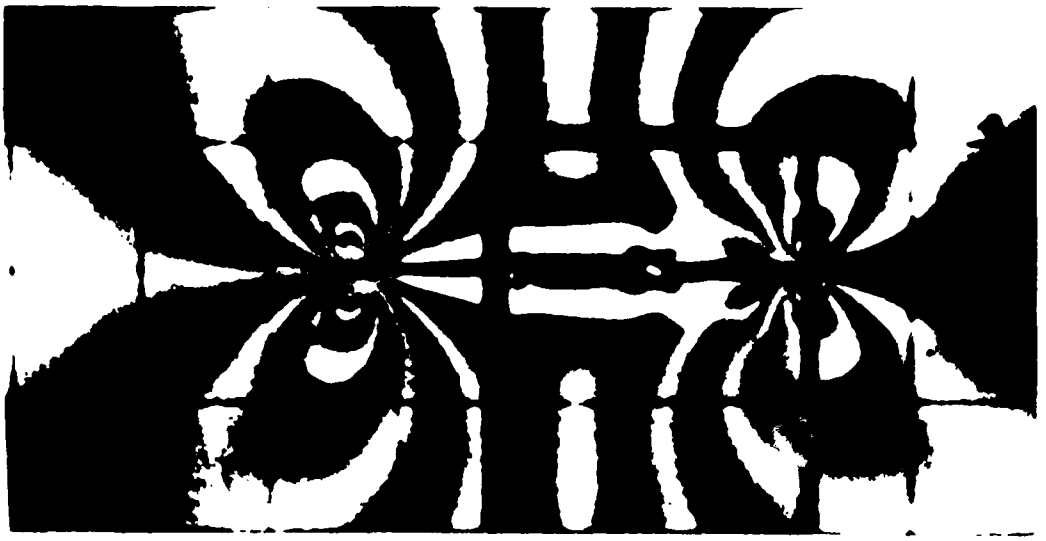

Frame 1. 15 μseconds

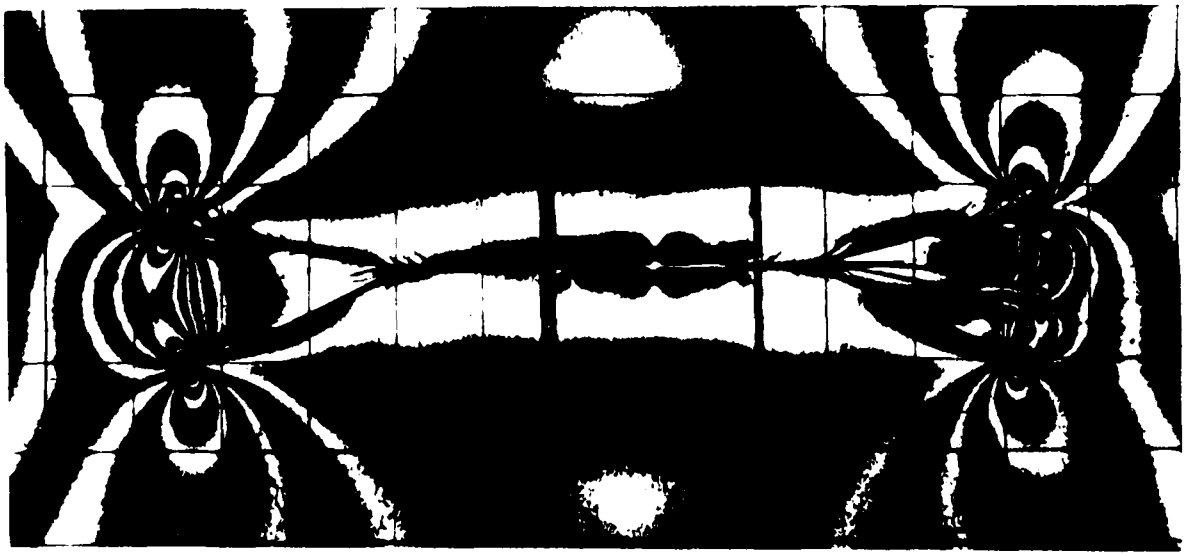

Frame 13. 195 μseconds

Figure 8. [illegible] Isochromatic Patterns of Crack Propagation in Homalite-100. Specimen No. MD012884 Bottom

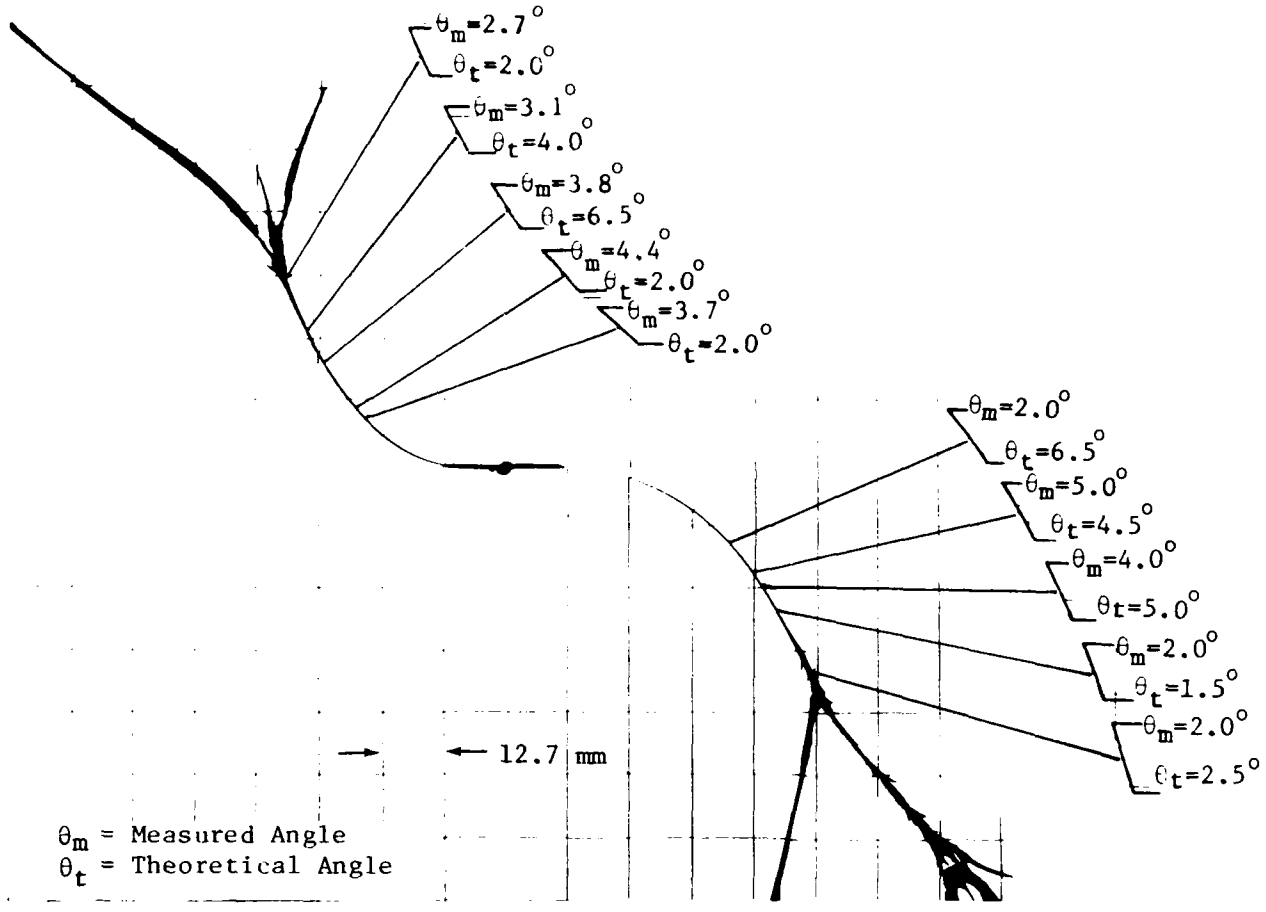

Figure 7. Crack Curving and Crack Branching of Specimen No. DH072084. B=1.6

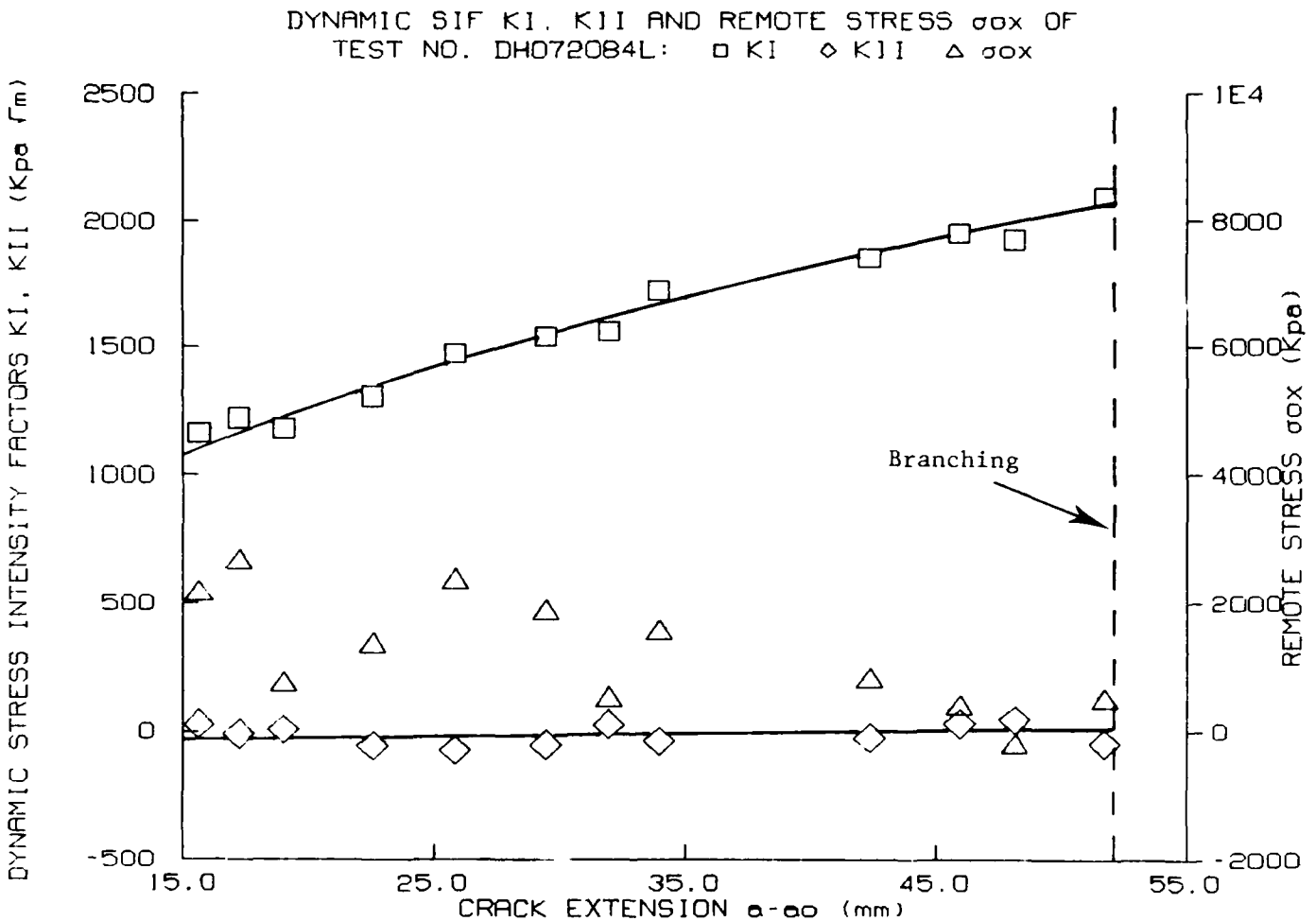

Figure 6b. K_I, K_{II} and σ_{ox} Variations Along Left Crack

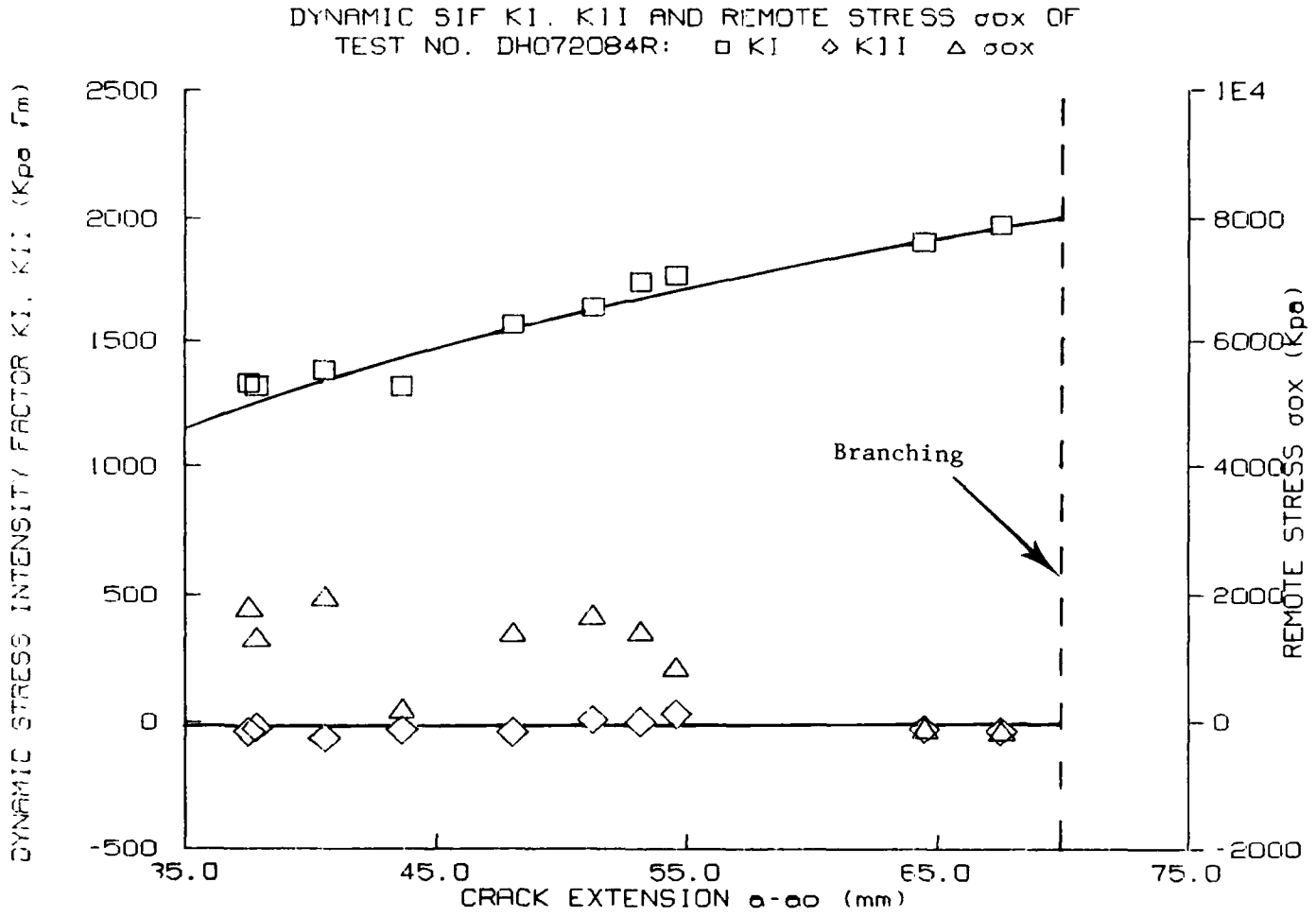

Figure 6a. K_I, K_{II} and σ_{ox} Variations Along Right Crack

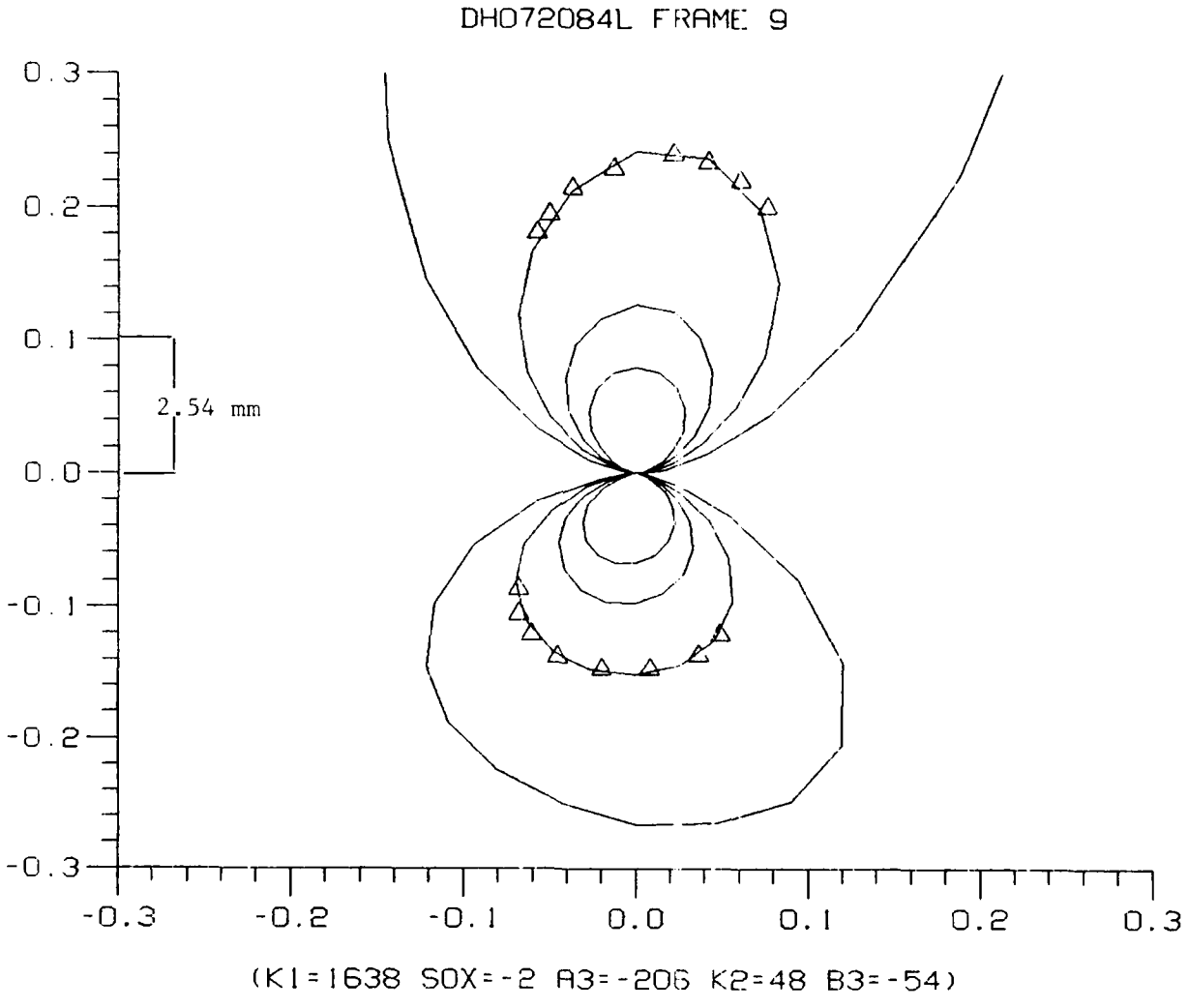

Figure 5b. Data Points and Reconstructed Isochromatics Pattern of a Curved Crack Specimen No. DH072084 Frame No. 9

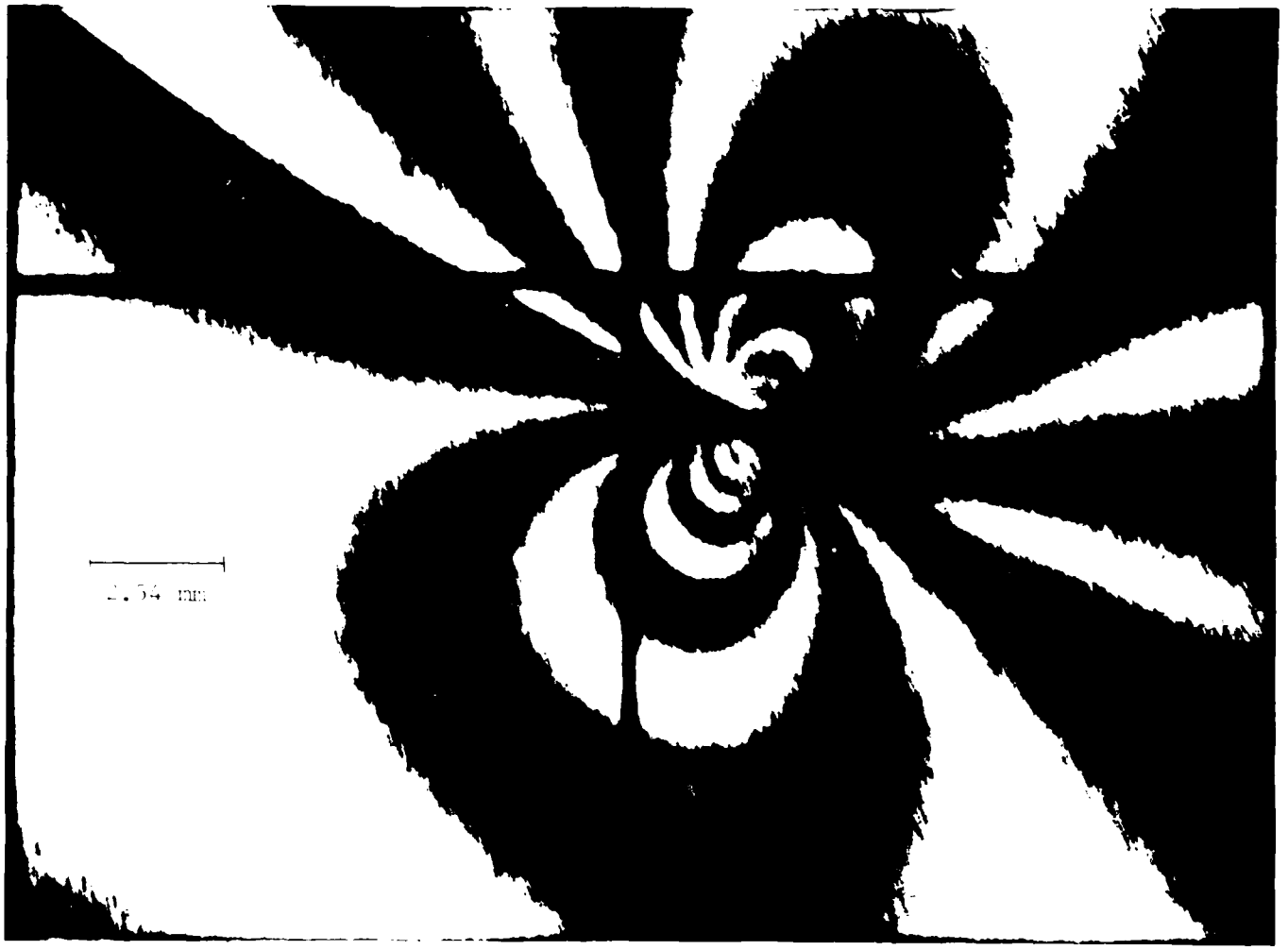

Figure 5a. Dynamic Isochromatic Pattern of a Curved Crack Specimen No. DH072084 Frame No. 9

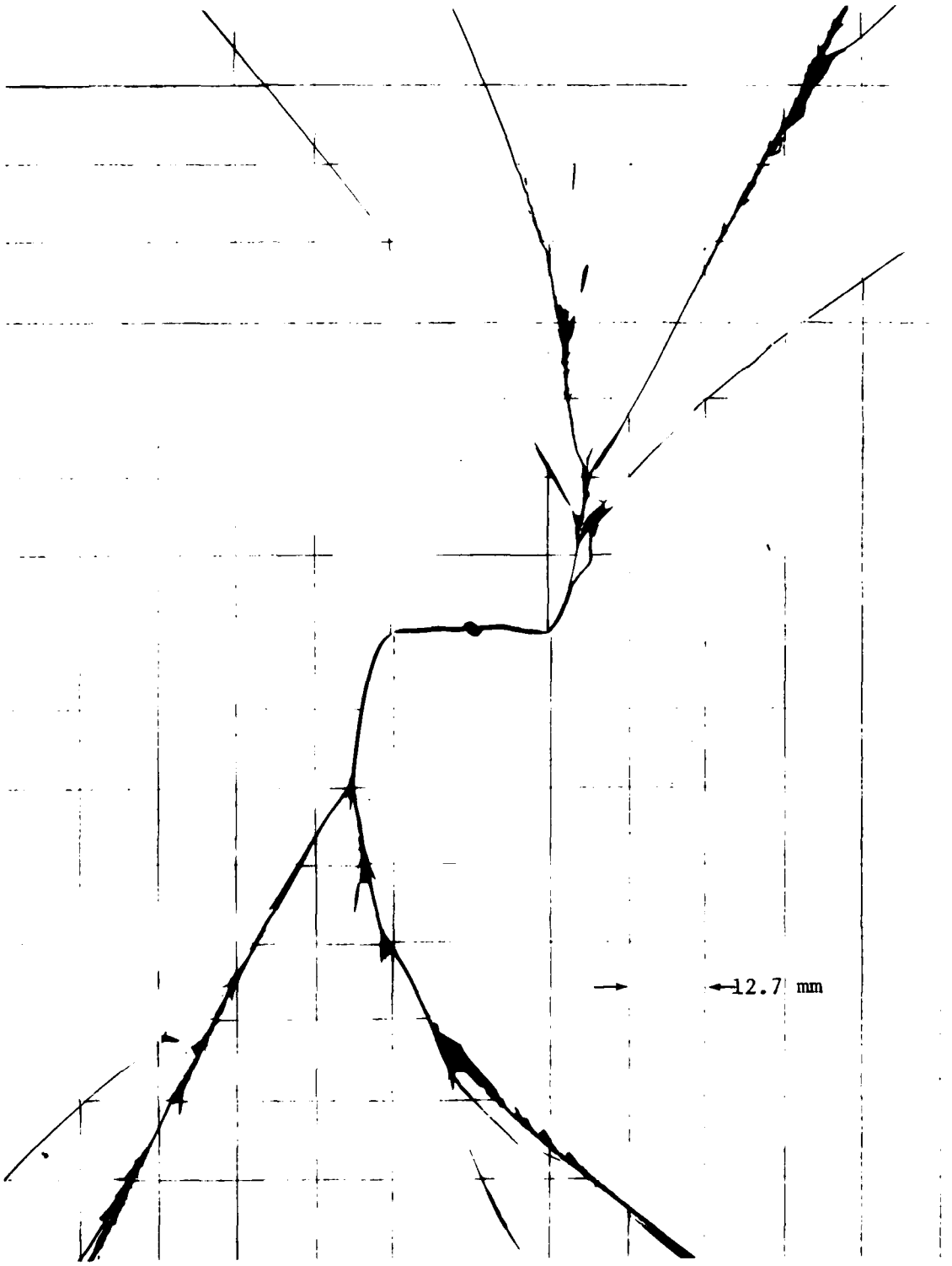

Figure 4. Cruciform Homalite-100 Specimen Test No. DH071784 Biaxial Load Ratio B=3.05

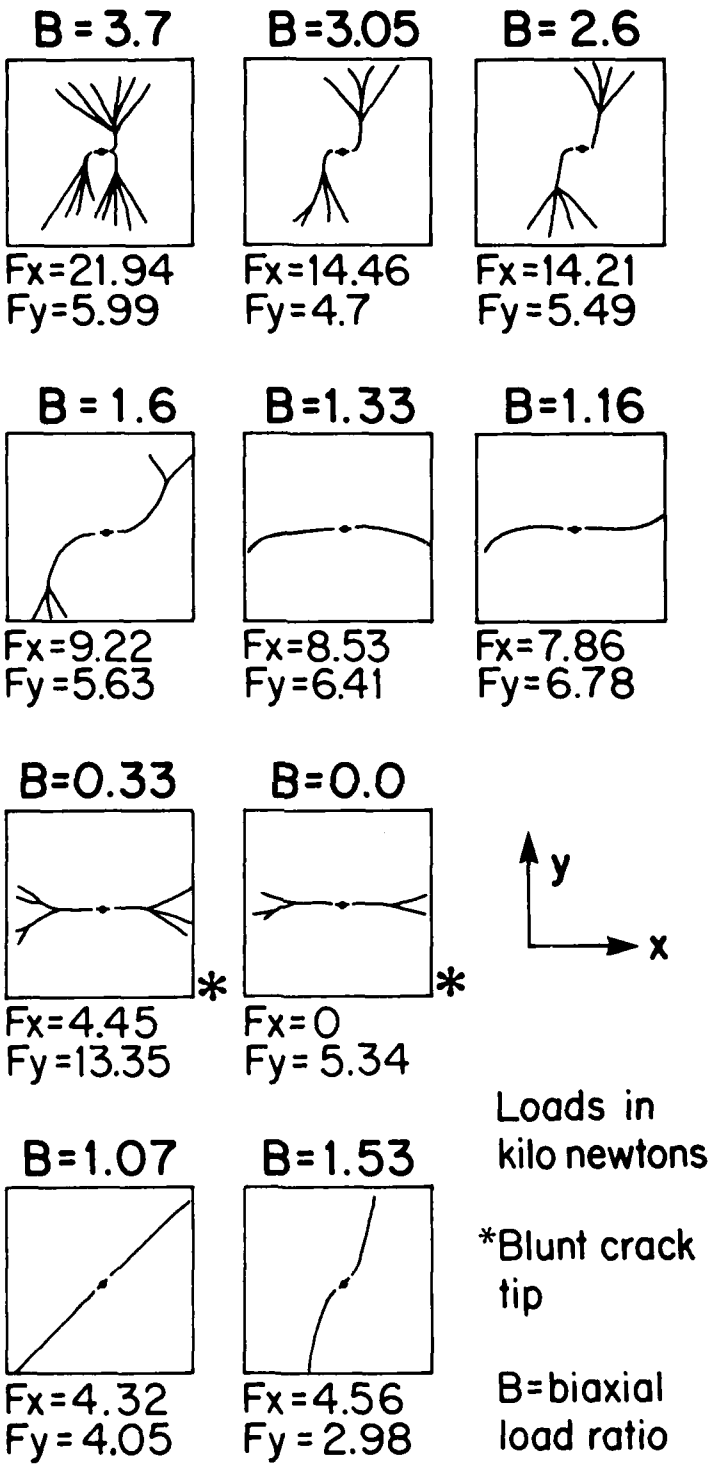

Figure 3. Crack Trajectories Under Biaxial Loadings in 16.4 mm Thick Homalite-100

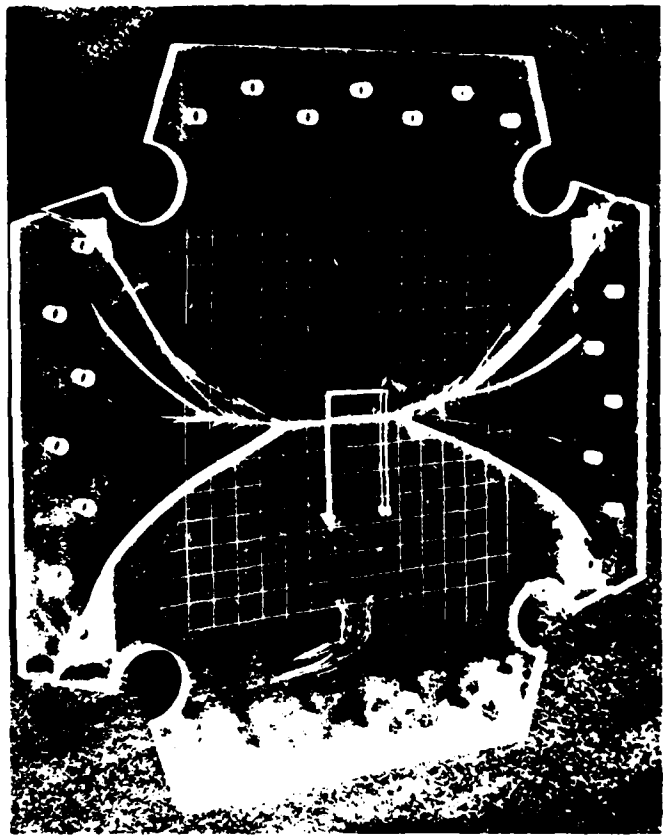

Figure 2. Cruciform Specimen Test No. MD012884 B=0.33

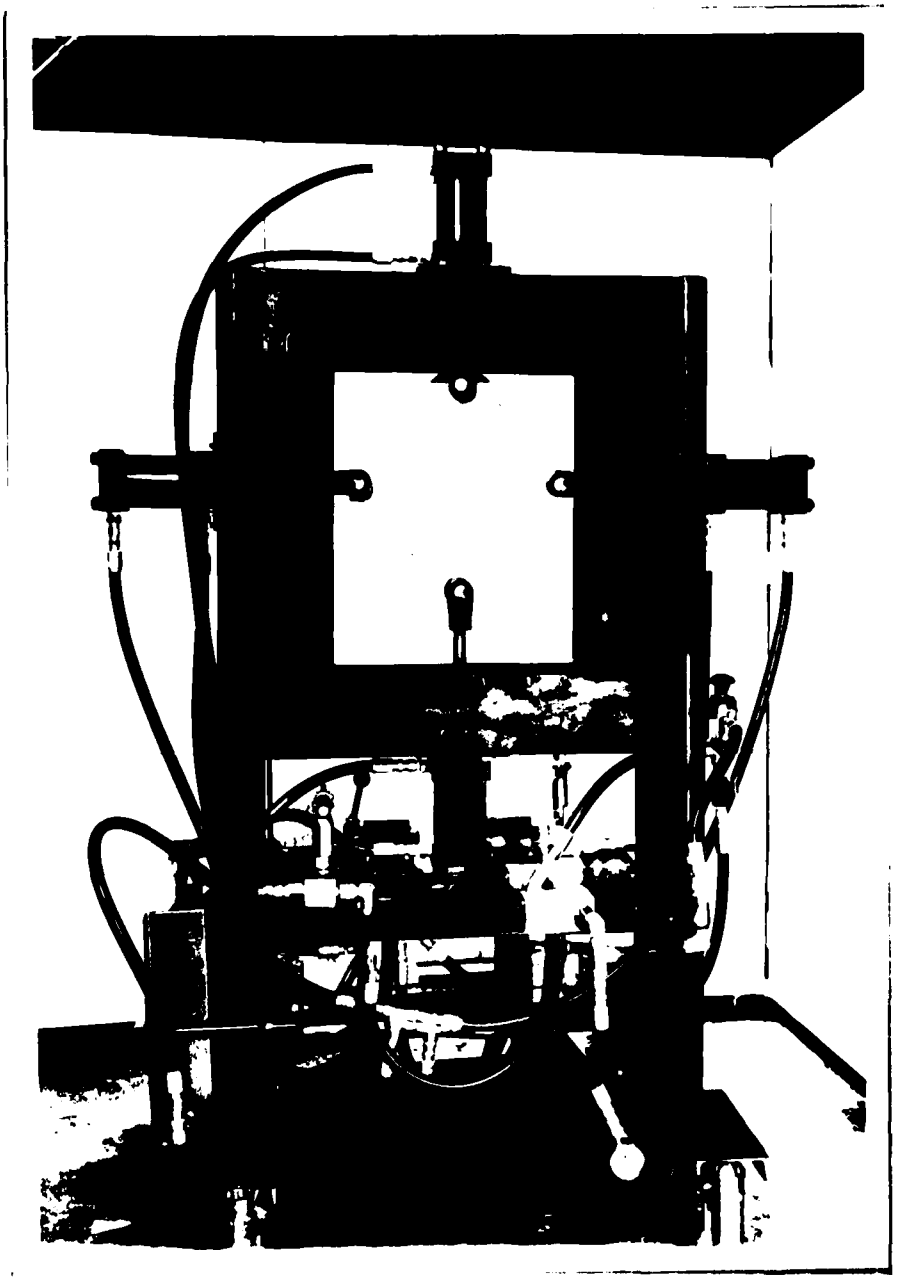

Figure 1. Tension/Compression Biaxial Testing Machine

END

FILMED

4-85

DTIC